OPEN ACCESS
Journal of Multidisciplinary Applied Natural Science Vol. 2 No. 2 (2022) https://doi.org/10.47352/jmans.2774-3047.126

Research Article

Removal of Toxic Cations from Aqueous Solutions using Ginger Root Waste

Jude Chinedu Onwuka*, Stephen Igberi Azubuike, and Timothy M. Akpomie

Received : April 4, 2022 | Revised : May 26, 2022 | Accepted : May 28, 2022 | Online : May 29, 2022

Abstract

Recently, the harmful impact of toxic metals in the aquatic environment cannot be over emphasized again. This work investigated the potential application of ginger root waste (GRW) to remove toxic cations (Cd^{2+} and Pb^{2+}) from the aqueous medium. Batch adsorption examination was carried out as a function of sorbent dose, initial metal ion concentration, contact time, and temperature. The sorption equilibrium of the metal ions onto the GRW was subjected to Langmuir, Freundlich, Elovich and Redlich-Peterson isotherm models over concentration ranges of 10-50 mg/L. Sorption information was used for kinetic and thermodynamic modeling. The GRW materials before and after sorption was characterized using FTIR and SEM. Results showed higher removal percentage of Cd^{2+} over Pb^{2+} ions in all the factors studied. The Redlich – Peterson isotherm model affirmed that sorption of Cd^{2+} and Pb^{2+} occurred in a heterogenous surface of the sorbent which is strongly influenced by multiple micropores and caves. Kinetic studies revealed that the sorption was controlled through intra-particle diffusion model aided by surface and chemical reactions. Meanwhile, thermodynamic parameters indicated that the Cd^{2+} and Pb^{2+} sorption process was endothermic, however, non-spontaneous at temperature of 303 and 313 K. The FTIR and SEM data showed the evidence of successful sorption of the toxic cations on to the sorbent material.

Keywords: Ginger root waste, sorption, toxic cations, kinetics, thermodynamics

1. INTRODUCTION

Heavy metal contamination is a serious challenge to the human race and the natural ecosystem. The environmental hazard and their effects on human existence are very serious [1] due to their accumulation in the human body and inability to biodegrade into harmless waste [2]. Today, the dangerous global impact of these metals on the ecosystem has become a non-push-over reality that is very difficult to be circumvented. Environmental pollution by heavy metals occurs by means of industrialization and extraction of natural resources [3]. Most industrial discharge and effluent contain high amounts of heavy metals which consequently constitute serious concern due to the high toxicity it portends to the living organism [4]. Organic wastes are quite susceptible to biodegradation, but heavy metals are not simply degraded by any biological means into harmless by-products [2].

The global increase in industrialization has accelerated industrial applications of heavy metals mainly as the catalyst and thus, increased their presence in wastewater giving rise to environmental pollution and wastewater contamination. Among the heavy metals, cadmium and lead, which are quite carcinogenic, are often found in industrial effluents such as those related to mining, metallurgy, petrochemicals, electroplating, batteries, pharmaceutical industries, paper, pulp, plastic, and paint manufacturing [5]. These metals are presumed toxic since they are not metabolized by the human body rather, they keep accumulating in the human tissues [6]-[9]. Thus, it becomes incumbent to search for the possible way of removing these toxic metals from the aqueous medium.

As a result of the many health challenges associated with contamination of water bodies by heavy metals, a lot of techniques such as chemical precipitation, ion exchange, electro-dialysis, membrane separation, and nanofiltration have been implored in preventing the presence of metal cations in our drinking water samples. However, there are obvious limitations inherent with the application of these techniques [10] including less efficiency and sensitivity, generation of sludge, high maintenance cost, high energy and reagent requirement, and inability to sequestrate metal ions at low concentration [11]. These limitations

Table 1. Data isolated from equilibrium adsorption isotherm plots.

Toxic cation	Langmuir Isotherm				Freundlich Isotherm			Elovich Isotherm			Redlich-Peterson		
	q_{max}	*b*	R_L	R^2	K_f	n	R^2	q_m	Ke	R^2	*β*	*A*	R^2
Cd^{2+}	-0.9832	-0.1709	0.8562	**0.7691**	0.0463	0.3493	**0.9640***	-3.2927	1.5095	**0.8868**	1.8622	0.0463	**0.9187**
Pb^{2+}	4.0016	0.0646	0.7946	0.0045	11.1970	-1.0092	0.0495	1.6292	5.4016	**0.9817***	1.9906	11.1931	0.1735

Note: * means highest R^2 values. R^2 values that are moderate are bolded

prompted individuals and research institutes to engage themselves in finding the best viable technique to adequately bring this menace into limits acceptable by standard organizations and one of such options is well provided in the adsorption process [12]. The adsorption process is cheap, eco-friendly and cost-effective as this process does not produce sludge and does not require high energy and reagents [10][11].

Globally, safe drinking water is everyone's concern, as it is difficult to find anybody who has not been affected by waterborne ailment [13]. Termed as a “universal solvent”, a higher percentage of the global population depends on water for drinking and domestic uses [10]. Due to the indispensable daily need and use of water across the globe, it has been made vulnerable and susceptible to being contaminated by the heavy metal discharge of domestic and industrial effluents, radioactive waste, mining waste, leakages from oil pipelines and atmospheric deposition [14]. Consequently, this has made water one of the key sources of global infection and diseases [15]. Statistics show that 80% of diseases and infections globally are waterborne and there is the propensity that it will be doubled if nothing is done in the near future [16]. At the moment, the global concern on heavy metal accumulation in drinking water and its effects on the human body is on the increase. The apprehension is that no biological means of degradation have been identified for these set of elements [3].

Health experts opined those natural products such as ginger drink are of great benefit to the human body [17]. Recent discoveries showed that it prevents nausea and vomiting, muscle pain and curbs cancer growth, soothes sore throat, and prevents common cold [18][19]. Nutritionally, the ginger drink is rich in antioxidants which are necessary for combating activities of free radicals in the body [12]. According to Adanlawao and Dairo [20], the ginger drink is quite rich in potassium, an important mineral for biochemical reactions in the body. Chronic intake of synthetic beverages majority of which are soft drinks is susceptible to dental erosion, obesity with a high risk of cardiovascular dysfunction and type 2-diabetes [18]. Due to these obvious health concerns on synthetic drink consumption, the focus has been shifted towards the consumption of natural drinks such as ginger root drinks [21]. Unfortunately, after the aqueous extraction of the ginger root, the wastes are dumped indiscriminately, thus, constituting an environmental nuisance. Previous research [12] utilized ginger root in removing selected toxic metal cations. However, this research aims to study the potential of using ginger root waste (GRW) to specifically remove Cd^{2+} and Pb^{2+} from the aqueous solution.

2. MATERIALS AND METHODS

2.1. Sample Collection and Preparation

The fresh ginger roots used for this research (201 g) were obtained from the Lafia main market, in Nasarawa State. It was transported in a polyethylene bag to the Department of Chemistry Laboratory, Federal University of Lafia. It was washed and rinsed severally with deionized water to remove dust and adhering soil particles. The thin outer covers were carefully peeled using stainless steel knife. The sample was washed again and sliced into bits and pounded using a ceramic mortar. The pounded sample was placed in a stainless basin, and 2 L of deionized water was added. The mixture was allowed to stand for 10 min, stirred and then filtered. The residue obtained after the juice extraction was re-soaked in 2 L of deionized water for another 10 min. This process was repeated for further three consecutive times and filtered after each soaking. The chaff obtained after this series of extraction is referred to as the ginger root waste. The waste was air-dried for 24 h and then oven-dried for 72 h at 80 °C. The dried sample was ground into fine powder using ceramic mortar and pestle and sieved to less than 1 mm fine particle size with a sieve and stored in a plastic sealable bag ready for the chemical analysis.

2.2. Batch Sorption Studies

The experimental solution was prepared by diluting the stock solution earlier prepared with deionized water. A 50 mL portion of the prepared 10 mg/L metal ion solution was measured into 250 mL plastic container and 0.5 g of the sorbent (GRW) was added. The plastic container was closed and then placed on a shaker (Bernareggio MI, PID system type M 428-Bd) with a temperature-controlled water bath. It was shaken continuously for 60 min at 27 °C and 120 rpm. The supernatant was filtered using 0.2 mm Whatman filter paper. The filtrate was analyzed using atomic absorption spectrophotometry (PG990) in order to ascertain the equilibrium metal ion concentrations. Various parameters of the adsorption process were studied as a function of sorbent dose, initial metal ion concentration, contact time and temperature of the solution. The effect of sorbent dose (0.5, 1.0, 1.5, 2.0, and 2.5 g) was studied by fixing the volume (50 mL) and concentration (10 mg/L) of toxic cations as well as the contact time (60 min) and temperature (27 °C). The effect of initial metal ion concentration (10, 20, 30, 40, and 50 mg/L) was carried out by metal ions sorption at a constant sorbent dose, contact time and temperature. The contact time effect (30, 60, 90, 120, and 150 min) was studied under various temperatures (303, 313, 323, and 343 K) while keeping other factors constant. Similarly, the variation of temperature (303, 313, 323, and 343 K) was carried out at various contact times (30, 60, 90, 120 and 150 min). The amount of metal ion sorbed per unit mass was calculated using a mass balance as shown Eq. 1.

$$q_e = \frac{\text{Ci} - \text{Ce}}{\text{m}} \text{ x v} \qquad \textbf{(1)}$$

Where q_e is heavy metal ion concentration absorbed onto the sorbent at equilibrium (mg/g), C_i and C_e are initial and equilibrium concentrations (mg/L) of the metal ions, respectively, m is mass (mg) of sorbent, and V is the volume (L) of sorbate solution.

The adsorption or removal percentage (%) was calculated using Eq. 2.

$$\%\ \text{Removal} = \frac{\text{Ci} - \text{Ce}}{\text{Ci}} \text{ x } 100 \qquad \textbf{(2)}$$

2.3. Adsorption Isotherm Modeling

This experiment was used to establish the relationship between the amount of the toxic cations (Cd^{2+} and Pb^{2+}) that was adsorbed by the GRW sorbent GRW and the equilibrium concentrations of the toxic cations at a constant temperature [12]. Langmuir, Freundlich, Elovich and Redlich-Peterson isotherm models were used to evaluate how the toxic cations (adsorbate) interacted with the GRW sorbent. This study was conducted by fitting the obtained data from the effect of initial metal ion concentration into the isotherm models.

2.3.1. Langmuir Isotherm

The equation was developed by Irving Langmuir (1916). The linearized form of the Langmuir model as shown in Eq. 3, was used in this study.

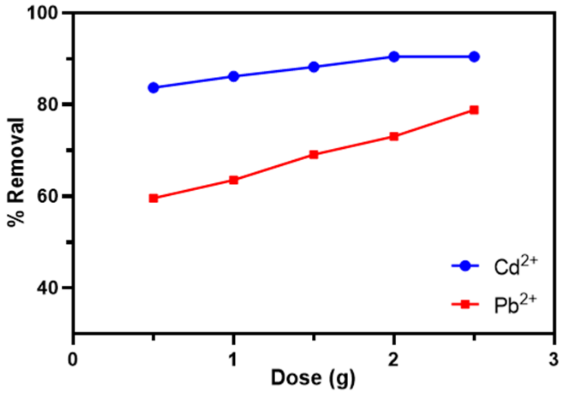

Figure 1. Effect of sorbent dose on Cd^{2+} and Pb^{2+} sorption.

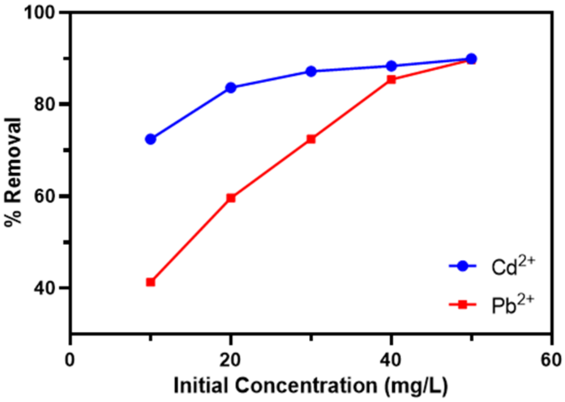

Figure 2. Effect of initial metal ion concentration on Cd^{2+} and Pb^{2+} sorption.

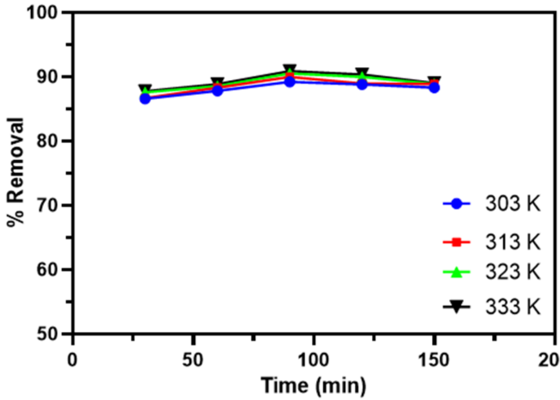

Figure 3. Effect of contact time for Cd^{2+} sorption at various temperatures.

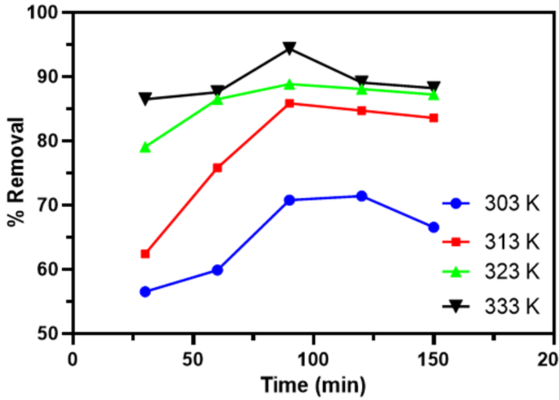

Figure 4. Effect of contact time for Pb^{2+} sorption at various temperatures.

$$\frac{Ce}{qe} = \frac{1}{b \times qmax} + \frac{1 \times Ce}{qmax} \tag{3}$$

Where C_e is concentration at equilibrium or final concentration of the metal in solution (mg/L), q_e is adsorption efficiency or the amount of the adsorbate adsorbed at equilibrium (mg/g), q_{max} is the maximum adsorption capacity (mg/g), and b is the Langmuir constant related to the energy of adsorption (L/mg). A plot of the graph C_e/q_e against C_e, produces $1/q_{max}$ as the slope, and thus, q_{max} was calculated. The value of b which is the Langmuir constant was evaluated from the intercept of the graph which is $1/b$ x q_{max} [22].

Dimensionless equilibrium function known as R_L value was evaluated using Eq. 4 expressed as:

$$R_L = \frac{1}{1 + b \times qmax} \tag{4}$$

When $R_L = 1$, a linear adsorption occurred. If $R_L = 0$, there is a irreversible adsorption. But when $0 < R_L < 1$, then a favorable adsorption occurred.

2.3.2. Freundlich Isotherm

The linear form of Freundlich isotherm demonstrated in Eq. 5, was applied.

$$\log q_e = \log k_f + \frac{1}{n} \log C_e \tag{5}$$

A plot of $logq_e$ against $logC_e$ produced $1/n$ as the slope, from where n was evaluated, while from the intercept ($logk_f$), k_f was estimated. It should be noted that k_f and n are Freundlich constants related to adsorption capacity and adsorption intensity, respectively [23].

2.3.3. Elovich Isotherm

The linear form of Elovich isotherm used is given as Eq. 6.

$$\frac{\text{Inq}_e}{C_e} = \text{InK}_e q_m - \frac{q_e}{q_m} \tag{6}$$

The plot of $\frac{\text{Inq}_e}{C_e}$ against q_e gives a straight line. Thus, Elovich maximum adsorption capacity (q_m) and Elovich constant (K_e) were calculated from the slope ($\frac{1}{q_m}$)and intercept ($\text{InK}_e q_m$), respectively.

2.3.4. Redlich-Peterson Isotherm

The linear form of the Redlich-Peterson isotherm used is shown in Eq. 7.

$$ln\frac{C_e}{q_e} = \beta lnC_e - lnA \tag{7}$$

Where A is the Redlich-Peterson isotherm constant (L/g), β (L/mg) is the exponent, C_e (mg/L) is the liquid-phase equilibrium concentration of the sorbent (GRW) while q_e is the sorbate (Cd^{2+} and Pb^{2+}) equilibrium onto the GRW sorbent. When the graph of InC_e/q_e vs InC_e is plotted, the slope is β while the intercept is lnA. When β value is below or equal to 1, the Redlich-Peterson isotherm is confined to Langmuir isotherm, however, when β value is above 1, the Redlich-Peterson isotherm tends to Freundlich isotherm. The constant "A" indicates the sorption capacity [24][25].

2.4. Kinetic Studies

This was studied to measure the uptake of the toxic cations as a function of time at a constant concentration so as to determine the mechanism or reaction pathway involved in the toxic cation uptake by the sorbent. Thus, data obtained from the effect of contact time were analyzed using pseudo–first order, pseudo–second order, intra–particle diffusion and liquid film diffusion models.

2.4.1. Pseudo First–Order kinetic

Pseudo first-order kinetic was carried out to establish the contribution of physisorption or surface reaction, to the uptake of the toxic cations by the sorbent. According to Amadi et al. [26], the linear form of pseudo first–order kinetics is given below.

$$\log(q_e - q_t) = \log q_e - \frac{K_1 \times t}{2.303} \quad \textbf{(8)}$$

The plot of $log(q_e\text{-}q_t)$ against time 't', gave - $\frac{K_1}{2.303}$ as the slope and $logq_e$ as the intercept [27].

2.4.2. Pseudo Second–Order Kinetic

The contribution of chemisorption was evaluated by analyzing the data with pseudo-second order kinetic model. The linear form of the pseudo-second order kinetic is stated Eq. 9.

$$\frac{1}{q_e - q_t} = \frac{1}{q_t} + k_2 t \quad \textbf{(9)}$$

The plot of $\frac{1}{q_e - q_t}$ against t, gives k_2 as the slope and $\frac{1}{q}$ as the intercept.

2.4.3. Intra–Particle Diffusion

The equation for the linear form of intra-particle diffusion kinetics is given Eq 10.

$$q_t = k_d \times t^{1/2} + C \quad \textbf{(10)}$$

Thus, when q_t is plotted against $t^{1/2}$, the slope is the rate constant k_d in (mg/(g min$^{1/2}$)) and the intercept 'C' in (mg/g). The importance of the intercept is that it explains the thickness of the boundary of the layer. The characteristic significance of the value of the constant 'C' is that the larger the value, the greater the boundary layer thickness [22][27].

2.4.4. Liquid–Film Diffusion

This was used to investigate the rate at which the toxic cations in the form of a film glide over one another [25]. The linear form of liquid film diffusion model is given below.

$$\text{In}(1\text{-}\alpha) = k_{lf}t + C \quad \textbf{(11)}$$

Where $\alpha = q_t/q_e$, k_{lf} is the liquid film diffusion rate constant. A plot of $In(1\text{-}\alpha)$ against time (t) yields the constant k_{lf} (min^{-1}) as the slope and a dimensionless constant C as the intercept [27].

2.5. Thermodynamic Studies

Thermodynamic parameters such as enthalpy change (ΔH), entropy change (ΔS), and Gibbs' free energy (ΔG), of the adsorption processes were determined. The Arrhenius equation described by Onwuka et al. [27], was used for the thermodynamic modeling, the equation is expressed in Eq. 12.

$$\ln q_T = -\frac{\Delta H}{RT} + \frac{\Delta H}{RT_0} + \ln q_0 \quad \textbf{(12)}$$

The enthalpy change (ΔH) was determined from the slope of the plot of lnq_T versus $1/T$ using Eq.12.

The heat capacity (Cp) and entropy change, (ΔS), were determined from Eqs. (13) and (14) respectively.

$$\Delta H = C_p(T_2 - T_1) \quad \textbf{(13)}$$

$$\Delta S = C_p \ln\frac{T_2}{T_1} + R\ln\frac{P_1}{P_2} \quad \textbf{(14)}$$

The Gibbs' free energy was determined using Eq. 15.

Table 2. ANOVA for effect of contact time on the sorption of Cd^{2+} and Pb^{2+} at various temperatures.

	Source of Variation	*SS*	*df*	*MS*	*F_{cal}*	*P-value*	*F_{crit}*
Cd^{2+}	Between Groups	10.46042	4	2.615106	0.005798	0.999927	2.866081
	Within Groups	9021.483	20	451.0741			
	Total	9031.943	24				
Pb^{2+}	Between Groups	2178.819	4	544.7049	1.127699	0.371616	2.866081
	Within Groups	9660.465	20	483.0232			
	Total	11839.28	24				

Table 3. ANOVA for effect of temperature for Cd^{2+} and Pb^{2+} sorption at different time intervals.

	Source of Variation	*SS*	*df*	*MS*	*F*	*P-value*	*F_{crit}*
Cd^{2+}	Between Groups	175150.1	5	35030.03	1247.75	3.31705E-22	2.772853
	Within Groups	505.3421	18	28.07456			
	Total	175655.5	23				
Pb^{2+}	Between Groups	189251.5	5	37850.31	277.7577	2.22831E-16	2.772853
	Within Groups	2452.877	18	136.2709			
	Total	191704.4	23				

$$\Delta G = \Delta H - T\Delta S \tag{15}$$

Where q_t is the amount adsorbed at temperature T, q_o is the amount adsorbed at temperature T_O, R is the universal gas constant, C_p is the heat capacity of the system at pressure p, P_1 and P_2 are the initial and final pressures respectively, T_1 and T_2 are the initial and final temperatures, respectively.

2.6. Characterization

2.6.1. Fourier Transform Infra-Red (FT-IR) Analysis

The KBr pellet was prepared by mixing about 1 mg of the sorbent with 250 mg KBr (FT-IR grade), pressed and placed for acquisition of IR spectrum on SHIMADZU model (8400S) of the FT-IR equipment. The spectra were recorded between 4000–400 cm^{-1} resolutions of 4 cm^{-1}. This was carried out at the National Research Institute for Chemical Technology (NARICT) Zaria, Kaduna State.

2.6.2. Scanning Electron Microscope (SEM) Analysis

The morphology of the GRW sorbent before and after metal ion sorption, was investigated using Scanning Electron Microscope (SEM; JSM-5610LV). The micrographs were taken at 1000 times magnification.

3. RESULTS AND DISCUSSIONS

3.1. Effect of Sorbent Dose

The result of the effect of sorbent dose on the metal ions (Cd^{2+} and Pb^{2+}) removal efficiency is presented in Fig. 1. The result shows that the sorption capacity is greatly influenced by the amount of sorbent material in the aqueous solution since the percentage sorption of the toxic metal ions increased in a higher sorbent dose. This suggests that there are more active binding sites, pores and caves at higher amount of the sorbent as similarly reported by Kampalanonwat and Supaphol [28] in a related investigation of heavy metal ion adsorption by animated polyacrylonitrile nanofibre mats. Increasing the sorbent dose also reduces the distance metal ions needed to travel in order to be entrapped by active pores and caves. A higher amount of the sorbent in solution results in a proportionate increase in the surface area which enhanced the sorption of more metal cations. A similar observation was reported by Vijayakurma et al. [29] and Shooto et al. [12] on natural pelite and ginger root, respectively. It was also observed in Fig 1 that increment in sorbent dose leads to higher Cd^{2+} adsorption through a maximum while Pb^{2+} adsorption increased continuously with the range of sorbent dose studied. This suggests that Cd^{2+} adsorption attained equilibrium faster than Pb^{2+} adsorption within the studied sorbent dosages. This can be attributed to the smaller ionic size of Cd^{2+} (compared to Pb^{2+}) which makes it more mobile and consequently results in more interaction with the active sites on the sorbent.

3.2. Effect of Initial Metal ion Concentrations

Fig. 2 shows the effect of initial metal ions concentration on the sorption of the toxic metal ions from the aqueous medium. It is observed that the removal of the metal ions increased with increase in the initial metal ions concentration. This suggests that at lower metal ion concentration, desorption of these metal cations from the sorbent occurs more than their adsorption on the sorbent. It also indicates that the metal ions interacted more with the sorbent active binding sites and caves at their higher metal ion concentrations compared to lower metal ion concentrations [30]. This can also imply that the ionic orientation favours sorption at higher initial metal ions concentration which is ascribed to the fact that the force of repulsion at higher concentrations has a minimum barrier to the sorption of the metal cations [31].

It was also observed in Fig. 2 just as in Fig. 1, that the sorption of Cd^{2+} from an aqueous medium was higher than that of Pb^{2+}. This disparity can be attributed to the differences in the atomic/ionic radius between the two toxic cations. Egila et al. [32], in similar research on *Amarathus hydridus* L. stalk waste, reported that atoms with lower atomic radii show more tendencies to be sorbed easily than atoms with larger atomic radii. The atomic radii of Cd^{2+} is 0.97 Å while that of Pb^{2+} is 1.20 Å. Thus, this made it relatively difficult for Pb^{2+} ions to infiltrate the lignocellulosic matrix component of the GRW sorbent and hence, result in lower Pb^{2+} sorption compared to Cd^{2+} sorption. Chukwuemeka et al. (2015), Onwuka et al. [27] and Shooto et al. [12] reported similar findings in their works on ginger, *Delonix regia* pods and ginger root, respectively.

3.3. Adsorption Isotherm Studies

The nature of the interaction between the toxic cations and the sorbent was assessed using Langmuir, Freundlich, Elovich and Redlich–Peterson isotherm models. Parameters evaluated and isolated from the isotherm plots in Equations 3, 5, 6 and 7 are summarized in Table 1. Generally, the value of coefficient of determination (R^2) in Table 1 shows that the order of best fit isotherm model for Cd^{2+} sorption onto the GRW sorbent is Freundlich > Redlich–Peterson > Elovich > Langmuir isotherm while that of Pb^{2+} sorption is Elovich > Redlich–Peterson > Freundlich > Langmuir isotherm.

R_L value is the most important feature of the Langmuir adsorption isotherm that helps to explain and predict the degree of interaction and compatibility between the sorbate and sorbent in the aqueous solution [22][33]. Favourable Langmuir isotherm modeling is such that $0<R_L<1$ as observed by Kussel et al. [34]. Thus, it was observed (Table 1) that the Langmuir dimensionless constant (R_L) values for Cd^{2+} and Pb^{2+} sorption from the aqueous medium, is less than 1 suggesting that the sorption of these toxic cations onto the GRW sorbent is relatively favourable. The high Langmuir R^2 value for Cd^{2+} sorption further supports this assertion. However, the low Langmuir R^2 value for Pb^{2+} sorption and the negative q_{max} for Cd^{2+} sorption which influenced the outcome of few other variables shown in Table 1, are indications that the application of Langmuir isotherm model alone cannot satisfactorily explain the sorption of Pb^{2+} and Cd^{2+} onto the sorbent [32][35][36].

In the Freundlich isotherm studies, the "*n*" value explains the degree of compatibility and interaction between the metal ions and the sorbent, while K_f is the adsorption capacity. The best fit "*n*" value for Freundlich adsorption isotherm is that value that

Table 4. Data Isolated from Kinetic Plots.

Temp (K)	Pseudo First–order			Pseudo Second–order			Intra–particle Diffusion			Liquid Film Diffusion			q_{exp}
	K_1	R^2	q_{cal}	K_2	R^2	q_{cal}	K_d	R^2	C	K_{lf}	R^2	C	
							Cd^{2+}						
303	0.012	0.086	0.132	0.540	0.282	-0.458	0.006	**0.583**[a]	1.769	0.011	0.069	2.506	1.847
313	0.009	0.072	0.145	0.264	**0.381**	0.278	0.006	**0.540**[a]	1.769	0.009	0.051	2.447	1.862
323	0.007	0.053	0.129	0.301	0.178	0.205	0.005	**0.383**[a]	1.794	0.008	0.040	2.542	1.874
333	0.007	0.050	0.132	0.291	0.157	0.204	0.005	**0.340**[a]	1.798	0.007	0.034	2.558	1.881
							Pb^{2+}						
303	0.000	0.004	0.205	0.026	0.002	0.081	0.040	**0.772**[a]	0.954	0.000	0.000	2.002	1.456
313	0.021	**0.470**	1.189	0.221	**0.480**	-0.135	0.065	**0.633**[a]	0.993	0.021	**0.375**	0.275	1.749
323	0.014	0.173	0.308	0.296	0.291	-0.879	0.022	**0.590**[a]	1.548	0.015	0.139	1.627	1.810
333	0.002	0.017	0.252	0.018	0.062	0.229	0.008	0.113	1.744	0.002	0.010	1.900	1.927

Note: [a] means highest R^2 values. R^2 values that are moderate are bolded

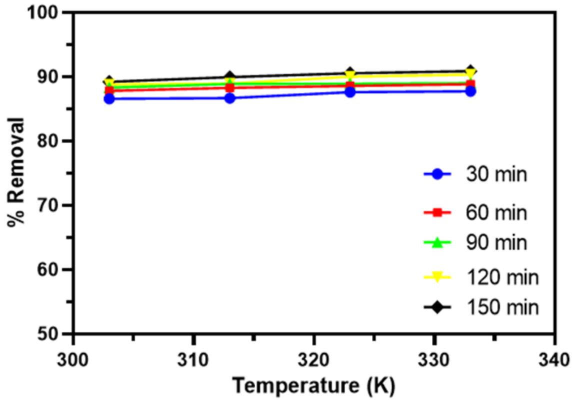

Figure 5. Effect of temperature for Cd^{2+} sorption at different contact time.

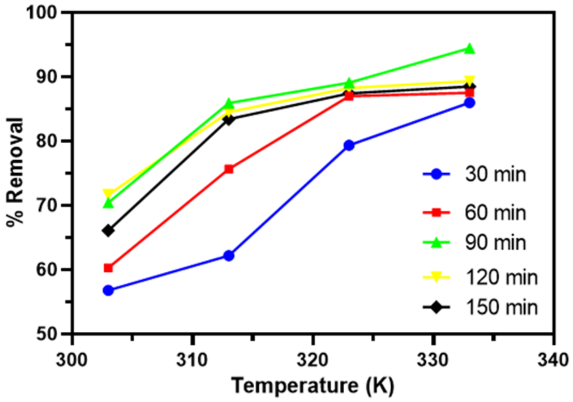

Figure 6. Effect of temperature for Pb^{2+} sorption at different contact time.

falls between 0 and 1 [37]. On this basis, it can be inferred that the sorption of Cd^{2+} onto the sorbent favourably aligned with the Freundlich isotherm modeling. This entails that the sorption is multilayer in nature and a physical process. This finding agrees with reports by Jimoh et al. [38], Amadi et al. [26] and Lei et al. [39] on Cd^{2+} adsorption using modified charcoal, cellulosic biosorbent derived from okra stem and modified biomass ash, respectively. The high R^2 value (Table 1) strengthens the assertion that Cd^{2+} sorption onto the GRW is favourable to the Freundlich isotherm. However, the negative "*n*" value of the Freundlich isotherm model for Pb^{2+} sorption implies that its sorption was quite difficult and the application of Freundlich isotherm model alone is inadequate to satisfactorily explain the sorption process. The difficulty in Pb^{2+} sorption could be attributed to its large ionic radius or the charge density [32]. This observation was opined by Alsenani [35] in similar research on *Calligonum comosum* leaf powder.

Table 1 further illustrates that Cd^{2+} and Pb^{2+} sorption onto the sorbent, aligned with the Elovich isotherm model based on their high coefficient of determination (R^2) values. This suggests that the sorption sites increased exponentially with adsorption validating that sorption of these toxic cations (Cd^{2+} and Pb^{2+}) is multilayer in nature [40]. It is therefore inferred that the sorption of Cd^{2+} and Pb^{2+} was dependent on the multiple micropores and the complicated chemical structure of sorbent. This was also reported by Achmad et al. [41] and Lei et al. [39] in similar works on a novel adsorbent developed from *Uncaria gambir* extract and adsorption of Cd^{2+} from aqueous solution by modified biomass ash.

Redlich–Peterson isotherm is used to correct the errors encountered in using Langmuir and Freundlich adsorption isotherm [42]. The model is actually the blend of Langmuir and Freundlich adsorption isotherms into one [24][43]. The Redlich –Peterson isotherm modeling for the Cd^{2+} sorption was also presented in Table 1. The high coefficient of determination (R^2) shows that Redlich-Peterson isotherm model satisfactorily predicted the sorption of Cd^{2+} onto the sorbent. It was also observed from Table 1 that the values of β for Cd^{2+} (1.8622) and Pb^{2+} (1.9906) sorption are above unity. This implies minimal or little influence of Langmuir adsorption isotherm on Cd^{2+} and Pb^{2+} sorption onto the sorbent. This assertion is anchored on the findings of Belhachemi and Addoun [24] that adsorption process where β approaches unity is suggestive that the sorption is best fitted to Langmuir isotherm model but if it is above unity, the sorption is best explained by the Freundlich isotherm model. Thus, it is inferred that the sorption of Cd^{2+} and Pb^{2+} satisfactorily aligned to Freundlich isotherm model.

Table 5. Thermodynamic data of Cd^{2+} and Pb^{2+} sorption.

Metal ion	C_p (J/K)	ΔH (J/mol)	ΔS (J/K)	ΔG (J/mol)	T (K)
Cd^{2+}	32.092	320.092	1.011	14.587	303
				4.477	313
				-5.633	323
				-15.743	333
Pb^{2+}	1267.636	12,676.365	39.931	577.260	303
				177.950	313
				-221.360	323
				-620.667	333

The implication is that the sorption of Cd^{2+} and Pb^{2+} occurred on a heterogeneous surface and is strongly influenced by multiple micropores, caves and rough surface morphology of the sorbent which constitutes the active sorption sites. This observation is validated by the strong agreement between the sorption capacities for Redlich–Peterson isotherm (A = 0.0463 for Cd^{2+} and 11.1931 for Pb^{2+}) and Freundlich adsorption isotherm (K_f = 0.0463 for Cd^{2+} and 11.1970 for Pb^{2+}) as shown in Table 1. Gimbert et al. [44] reported similar findings on catonized starch-based material in a single component system.

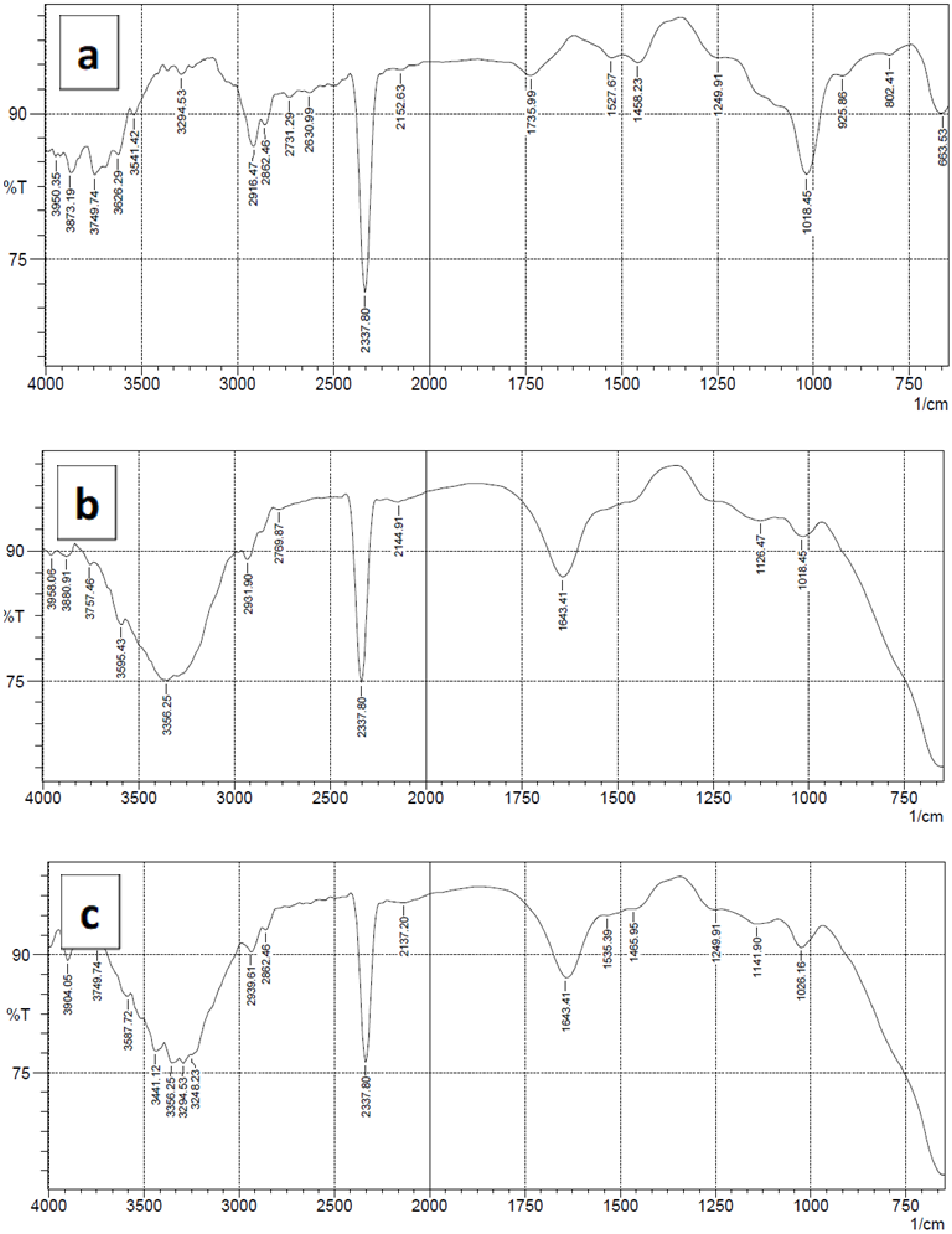

Figure 7. FTIR spectra of (a) unloaded (b) Cd^{2+} loaded and (c) Pb^{2+} loaded sorbents.

3.4. Effect of Contact Time at Various Temperatures

The effect of contact time on Cd^{2+} and Pb^{2+} sorption are shown Figs 3 and 4. The results show that the sorption of toxic metal ions (Cd^{2+} and Pb^{2+}) at various temperatures studied, increased through a maximum with increase in contact time (Figs 3 and 4). Thus, the sorption of toxic metal ions was very fast initially at the adsorbent-adsorbate contact until equilibrium (saturation) was attained at 90 min and then it gradually started decreasing despite the increase in the contact time. This is attributed to the saturation of the available pores, caves and adsorptive active binding sites. This observation was also reported by Vijayakumar et al. [29] in similar work on natural pelite.

It was further observed that a two-way adsorption process played out. First, was the rapid phase encounter that occurred between the time of the initial adsorbate-adsorbent contact to the time equilibrium was reached and the second phase was the slower phase that started from the time equilibrium was reached downward with declining adsorption even with increasing contact time. This is ascribed to the fact that at saturation point, all active sites, pores and caves are filled up and a further increase in the contact time results in desorption. This accounts for the decline in the sorption process after equilibrium has been reached, an ascertion also shared by Kekpugile et al. [10] in a related research on kinetic study of garlic and ginger. A similar inference was also opined by Kampalanonwat and Supaphol [28] in a related work on animated polyacrylonitrile nanofibre mats. Also, higher percentage removal of Cd^{2+} over Pb^{2+} was also observed (Figs 3 and 4). This is an indication that Cd^{2+} is more mobile and dynamic than Pb^{2+} in solution which is a function of the differences in the ionic size and charge density. Jimoh et al. [38] reported similar findings in related work on modified charcoal.

3.5. One–way factorial Analyses

Figs 3 and 4 showed the variations in the removal efficiency of Cd^{2+} and Pb^{2+} with contact time at different temperatures respectively. These variations in the removal efficiency of the toxic metal cations with time were tested for significant differences. The analysis of variance (ANOVA) presented in Table 2 shows that the observed variations in the sorption of Cd^{2+} and Pb^{2+} with contact time have no significant difference at the various temperatures studied. This is because the p-values are greater than $\alpha = 0.05$ and F_{cal} is less than $F_{crit.}$ Thus, it is a further validation of the null hypothesis. This result implies that any of the studied temperature can be used to explain/describe the variations of the metal ions sorption with contact time.

In Figs 5 and 6, the variations in the sorption of Cd^{2+} and Pb^{2+} with temperature at various contact time were shown. Table 3 shows that there is statistically significant difference in Cd^{2+} and Pb^{2+} sorption when the temperature was varied at different time. It can be concluded that at $\alpha = 0.05$, null hypotheses were rejected because F_{cal} is higher than F_{crit} and p-values is less than $\alpha = 0.05$. This is an indication that thermal influence is essential for the sorption of these metal adsorbates as was also observed by Batool et al. [45] in related study on linear and non-linear approach and error analysis.

3.6. Kinetic Studies

Reaction (pseudo first–order and pseudo second –order) and diffusion (Intra–particle and liquid film diffusion) kinetics were used to determine the sorption mechanism of the toxic cations (Cd^{2+} and Pb^{2+}) on the sorbent. The kinetic data extracted from the plots in Equations 7, 8, 9 and 10, are summarized in Table 4. The values of coefficient of determination (R^2), q_{cal} and q_{exp} for the various kinetic plots, were used to determine the mechanisms that contributed to the sorption of the toxic cations at each temperature. It was observed that pseudo first–order and pseudo second–order kinetic models could not satisfactorily explain the sorption process of the metal cations at all the temperatures studied (Table 4). This is because there is no strong agreement between the q_{cal} and q_{exp} values [22].

The values of coefficient of determination (R^2) within $0.43 \leq R^2 \leq 0.83$ are considered high and moderate [46]. The highest values of R^2 are obtained at intra–particle diffusion plots of all studied temperatures. Hence, diffusion into the pores of the GRW sorbent is the rate-controlling mechanism in the sorption of the toxic cations (Cd^{2+} and Pb^{2+}) at all the studied temperatures (303–333

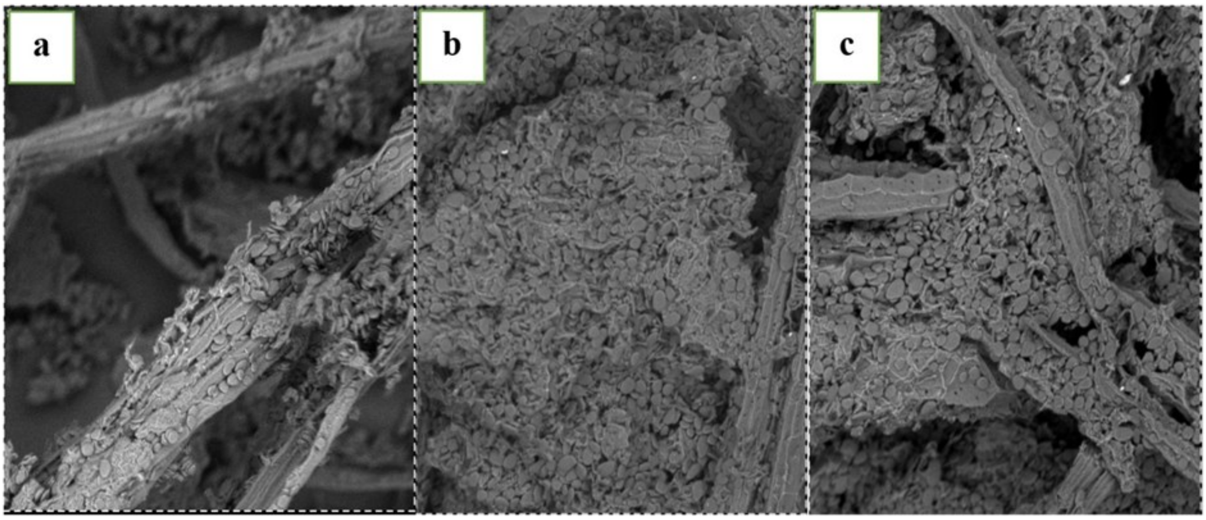

Figure 8. SEM Micrographs of (a) unloaded (b) Cd^{2+} loaded and (c) Pb^{2+} loaded sorbents.

K). However, intra–particle diffusion is not the sole mechanism in the sorption of these toxic cations because the linear plot did not pass through the origin [10][22]. It was also observed that chemical reaction contributed to the sorption mechanism of Cd^{2+} and Pb^{2+} at 313 K while surface reaction and transport of sorbate molecules from liquid to solid phase were majorly involved in Pb^{2+} sorption mechanism at 313 K. The intercepts obtained in the intra–particle diffusion plots are relatively high in all the sorption temperatures for Cd^{2+} sorption and at 323 K and 333 K for Pb^{2+} sorption. This indicates that the sorption process of these metal ions was mainly a surface reaction [26][27]. Other related studies that shared similar views are those of Ademiluyi and Ujile [47], Li et al. [48] and Kulkarni et al. [49].

3.7. Effect of Temperature at Different Time Intervals

The effect of temperature on the sorption Cd^{2+} and Pb^{2+} at different contact times by the sorbent is shown in Figs 5 and 6 respectively. The result indicated that the sorption of the toxic cations (Cd^{2+} and Pb^{2+}) increased steadily as the temperature was raised. This is attributed to the activated mobility of the metal cations introduced into the system by increase in temperature and also, the diffusion of the ionic species [38]. This is believed in facilitating the sorption of these toxic cations as demonstrated by the increase in percentage removal of the metal cations in the aqueous solution [50]. Therefore, thermal influence is opined to have a strong effect on the sorption of the metal ions. This was similarly reported by other kinetic studies by Wase [51] and Tounsadi et al. [36] for tea factory waste and *Diplotaxis hara glebionis corona* L.

3.8. Thermodynamic Studies

The data isolated from the thermodynamic plots using Equation 11, are summarized in Table 5. In the result, it was observed that the heat capacity of Cd^{2+} sorption onto the sorbent is 32.09 J/mol while that of Pb^{2+} sorption was 1267.636 J/mol. Heat capacity C_p is the quantity of thermal energy required to raise the temperature of adsorption by one degree [52]. The higher heat capacity of adsorption of Pb^{2+} can be attributed to the higher charge density of Pb^{2+} compared to Cd^{2+}. This is believed to have made it less mobile and so required higher thermal activation for the reaction to occur [38][53].

Table 5 further showed that the sorption of the metal cation was non-spontaneous at low temperatures of 303–313 K as depicted by the positive value of change in Gibbs free energy (ΔG). However, as the sorption temperature increased to 323–333 K, the values of ΔG for the metal cation sorption become negative suggesting that the meta cation sorption is spontaneous. The implication is that for sorption of these metal cations to occur onto the sorbent, heat must be added. This is ascertained by the positive value of enthalpy change (ΔH) which indicates that the sorption of these metal cations is endothermic in nature. Therefore, for the reaction (metal cation sorption) proceed, the initial energy barrier is required to be broken by increase in temperature. This is contrary to the findings of

Shooto et al. [12] but in agreement with findings of Kazi et al. [54], Hussein et al. [52] and Gabreslassie [55].

3.9. Fourier Transform Infra-red (FT-IR) Spectroscopy

The FTIR analysis of the unloaded, Cd^{2+} loaded and Pb^{2+} loaded sorbents, are presented in Fig 7a, 7b and 7c, respectively. The peak 2337.80 cm^{-1} appeared in both the unloaded and metal ions loaded sorbents. This peak falls within 2400-2000 cm^{-1} and thus, assigned to O=C=O stretching. The peak 1643.41 cm^{-1} as seen in Cd^{2+} and Pb^{2+} loaded sorbents (Fig 7b and 7c) falls within 1648-1638 cm^{-1} and is assigned to C=C stretching from alkene. The peak 1735.99 cm^{-1} falls within 1735-1750 cm^{-1} is assigned to C=O stretching. As the sorbent was hydrolysed during the metal ions sorption, the peak 3356.25 cm^{-1} appeared in both Fig 7b and 7c. This peak falls within the region 4000–3000 cm^{-1} which is assigned to O–H (stretching) resulting from ROH. This peak is very important in the investigation by virtue of the nature of sorbent used for the analysis. The GRW material is a plant fibre [56] and commonly fibre is a soluble polymer in solution containing hydrophilic groups such as the O–H groups that undergoes such a reaction mechanism that can entrap divalent cations [57]. Figs 7a, 7b and 7c show that during sorption, the bivalent toxic cations (Cd^{2+} and Pb^{2+}) interacted with the O–H, C=C and C=O groups which caused spectra enhancement/shift and also spectra appearance. The interaction between these functional groups and the bivalent toxic ions led to the sorption of these bivalent toxic cations [58][12].

3.10. Scanning Electron Microscope (SEM) Analysis

Figs 8a, 8b and 8c show the SEM micrographs of the unloaded, Cd^{2+} loaded and Pb^{2+} loaded sorbents, respectively. Pores, caves and roughened surfaces were observed in Fig 8a. These are factors suspected to facilitate and influence the sorption of Cd^{2+} and Pb^{2+} onto the sorbent [45][59]. Figs 8b and 8c show that after the sorption of the metal ions, there was conglutination of the neighboring fibres at the touching line making the morphology of the sorbent compact and the sorbent appeared smoother and slippery with tiny blocks depicting the distribution of the metal ions on the sorbent surface. This is evidence that sorption of these metal ions (Cd^{2+} and Pb^{2+}) onto the sorbent was successful which is in agreement with the previous studies [28][60].

4. CONCLUSIONS

This study showed that the ginger root waste (GRW) adsorbent material has the potential to remove toxic cations (Cd^{2+} and Pb^{2+}) from the aqueous medium. The GRW material was able to remove more Cd^{2+} from aqueous medium than Pb^{2+}. The sorption of these toxic cations occurred on a heterogeneous surface and is strongly influenced by multiple micropores, caves and rough surface morphology of the sorbent. Diffusion into the sorbent pores was pivotal for the sorption of these toxic cations. The sorption process is non–spontaneous at low temperature but spontaneous at higher temperature. The FTIR results showed that these toxic cations (Cd^{2+} and Pb^{2+}) were adsorbed at both hydrophilic and hydrophobic functional groups. SEM micrographs showed that the adsorption of these toxic cations changed the surface morphology of the GRW sorbent.

AUTHOR INFORMATION

Corresponding Author

Jude Chinedu Onwuka — Department of Science Laboratory Technology, Federal University of Lafia, Lafia – 950101 (Nigeria); Department of Chemistry, Federal University of Lafia, Lafia – 950101 (Nigeria);
orcid.org/0000-0003-2950-8273
Email: emperor20062003@yahoo.com

Authors

Stephen Igberi Azubuike — Department of Chemistry, Federal University of Lafia, Lafia – 950101 (Nigeria);
Timothy M. Akpomie — Department of Chemistry, Federal University of Lafia, Lafia – 950101 (Nigeria);

ACKNOWLEDGEMENT

The authors are immensely grateful to Mr. William Egbe and other staff and management of

National Soil Testing Laboratory Complex, Federal Ministry of Agriculture and Rural Development, Goningora, Kaduna State; for availing their laboratory services for this research.

REFERENCES

[1] M. A. Barakat. (2011). "New trends in removing heavy metals from industrial wastewater". *Arabian Journal of Chemistry*. **4** (4): 361–377. 10.1016/j.arabjc.2010.07.019.

[2] A. M. A. Al-Lami, S. R. Khudhaier, and O. A. Aswad. (2020). "Effects of heavy metals pollution on human health". *Annals of Tropical Medicine and Public Health*. **23** (11): 10.36295/asro.2020.231125.

[3] S. Sharma, S. Rana, A. Thakkar, A. Baldi, R. S. R. Murthy, and R. K. Sharma. (2016). "Physical, Chemical and Phytoremediation Technique for Removal of Heavy Metals". *Journal of Heavy Metal Toxicity and Diseases*. **1** (2): 20–28. 10.21767/2473-6457.100010.

[4] B. Bayat. (2002). "Comparative study of adsorption properties of Turkish fly ashes: I. The case of nickel(II), copper(II) and zinc (II)". *Journal of Hazardous Materials*. **95** (3): 251–273. 10.1016/S0304-3894(02)00140-1.

[5] M. Iqbal and R. G. J. Edyvean. (2005). "Loofa sponge immobilized fungal biosorbent: A robust system for cadmium and other dissolved metal removal from aqueous solution". *Chemosphere*. **61** (4): 510–518. 10.1016/j.chemosphere.2005.02.060.

[6] E. ul Islam, X. e. Yang, Z. li He, and Q. Mahmood. (2007). "Assessing potential dietary toxicity of heavy metals in selected vegetables and food crops". *Journal of Zhejiang University. Science. B*. **8** (1): 1–13. 10.1631/jzus.2007.B0001.

[7] D. C. K. Ko, J. F. Porter, and G. McKay. (2003). "Mass transport model for the fixed bed sorption of metal ions on bone char". *Industrial and Engineering Chemistry Research*. **42** (14): 3458–3469. 10.1021/ie020505t.

[8] C. Garbisu and I. Alkorta. (2001). "Phytoextraction: A cost-effective plant-based technology for the removal of metals from the environment". *Bioresource Technology*. **77** (3): 229–236. 10.1016/S0960-8524(00)00108-5.

[9] C. Gisbert, R. Ros, A. D. Haro, D. J. Walker, M. P. Bernal, R. Serrano, and J. N-Aviñó. (2003). "A plant genetically modified that accumulates Pb is especially promising for phytoremediation". *Biochemical and Biophysical Research Communications*. **303** (2): 440–445. 10.1016/S0006-291X(03)00349-8.

[10] K. Kekpugile, D. D., and J. I. Ndaka. (2019). "Kinetic Study of Garlic and Ginger Particles in Adsorption of Heavy Metals in Aqueous Solution". *Chemical and Process Engineering Research*. **60** (19): 136–141. 10.7176/cper/60-04.

[11] J. Salehzadeh. (2013). "Removal of Heavy Metals Pb2+, Cu2+, Zn2+, Cd2+, Ni2+, Co2+ and Fe3+ from Aqueous Solutions by using Xanthium Pensylvanicum". *Leonardo Journal of Sciences*. **12** (23): 97–104.

[12] N. D. Shooto, E. B. Naidoo, and M. Maubane. (2019). "Sorption studies of toxic cations on ginger root adsorbent". *Journal of Industrial and Engineering Chemistry*. **76** (20): 133–140. 10.1016/j.jiec.2019.02.027.

[13] M. Uyttendaele, E. De Boeck, and L. Jacxsens. (2016). "Challenges in Food Safety as Part of Food Security: Lessons Learnt on Food Safety in a Globalized World". *Procedia Food Science*. **6** : 16–22. 10.1016/j.profoo.2016.02.003.

[14] M. Mehra, B. Oinam, and C. K. Singh. (2016). "Integrated Assessment of Groundwater for Agricultural Use in Mewat District of Haryana, India Using Geographical Information System (GIS)". *Journal of the Indian Society of Remote Sensing*. **44** (5): 747–758. 10.1007/s12524-015-0541-6.

[15] S. Bibi, R. L. Khan, R. Nazir, P. Khan, H. U. Rehman, S. K. Shakir, S. Naz, M. A. Waheed, and R. Jan. (2016). "Heavy metals analysis in drinking water of Lakki Marwat District, KPK, Pakistan". *World applied sciences journal*. **34** (3): 15–19.

[16] M. J. Pawari and S. Gawade. (2015).

“Ground water pollution and its consequnces”. *International Journal of Engineering Research and General Science*. **3** (2): 773–776.

[17] A. Afkhami, T. Madrakian, A. Amini, and Z. Karimi. (2008). “Effect of the impregnation of carbon cloth with ethylenediaminetetraacetic acid on its adsorption capacity for the adsorption of several metal ions”. *Journal of Hazardous Materials*. **150** (2): 408–412. 10.1016/j.jhazmat.2007.04.123.

[18] D. Kregiel. (2015). “Health safety of soft drinks: Contents, containers, and microorganisms”. *BioMed Research International*. **2015** (15): 10–15. 10.1155/2015/128697.

[19] I. Onimawo. (2019). “Determination of Proximate and Mineral Composition of Three”. *ACTA science Nutritional Health*. **3** (7): 111–114.

[20] I. G. Adanlawo and . F. A. S. D. (2006). “Nutrient and Anti-nutrient Constituents of Ginger (Zingiber officinale, Roscoe) and the Influence of its Ethanolic Extract on Some Serum Enzymes in Albino Rats”. *International Journal of Biological Chemistry*. **1** (1): 38–46. 10.3923/ijbc.2007.38.46.

[21] J. M. Jones. (2014). “CODEX-aligned dietary fiber definitions help to bridge the ‘fiber gap’”. *Nutrition Journal*. **13** (1): 34. 10.1186/1475-2891-13-34.

[22] Z. Aly, A. Graulet, N. Scales, and T. Hanley. (2014). “Removal of aluminium from aqueous solutions using PAN-based adsorbents: characterisation, kinetics, equilibrium and thermodynamic studies”. *Environmental Science and Pollution Research*. **21** (5): 3972–3986. 10.1007/s11356-013-2305-6.

[23] J. X. Zhang and L. L. Ou. (2013). “Kinetic, isotherm and thermodynamic studies of the adsorption of crystal violet by activated carbon from peanut shells”. *Water Science and Technology*. **67** (4): 737–744. 10.2166/wst.2012.605.

[24] M. Belhachemi and F. Addoun. (2011). “Comparative adsorption isotherms and modeling of methylene blue onto activated carbons”. *Applied Water Science*. **1** (3–4): 111–117. 10.1007/s13201-011-0014-1.

[25] N. Ayawei, A. N. Ebelegi, and D. Wankasi. (2017). “Modelling and Interpretation of Adsorption Isotherms”. *Journal of Chemistry*. **2017** (17): 11–15. 10.1155/2017/3039817.

[26] O. K. Amadi, C. J. Odidizor, and I. A. Okoro. (2017). “sorption kinetic and intraparticle diffusivities of As 3+ and Hg 2+ Detoxification from Aqueous Solution Using Cellulosic Biosorbent Derived from Okra (Abelmoschus eaculentus) Stems”. *International Journal of Engineering Systems (IJEAIS)*. **1** (8): 75–85.

[27] J. C. Onwuka, E. B. Agbaji, V. O. Ajibola, and F. G. Okibe. (2016). “Kinetic studies of surface modification of lignocellulosic Delonix regia pods as sorbent for crude oil spill in water”. *Journal of Applied Research and Technology*. **14** (6): 415–424. 10.1016/j.jart.2016.09.004.

[28] P. Kampalanonwat and P. Supaphol. (2014). “The study of competitive adsorption of heavy metal ions from aqueous solution by aminated polyacrylonitrile nanofiber mats”. *Energy Procedia*. **56** (C): 142–151. 10.1016/j.egypro.2014.07.142.

[29] G. Vijayakumar, R. Tamilarasan, and M. Dharmendirakumar. (2012). “Adsorption, kinetic, equilibrium and thermodynamic studies on the removal of basic dye Rhodamine-B from aqueous solution by the use of natural adsorbent perlite”. *Journal of Materials and Environmental Science*. **3** (1): 157–170.

[30] H. Karimi (2017). “Effect of pH and Initial pb(II) Concentration on The Lead Removal Efficiency from Industrial Wastewater Using Ca(OH)2”. *International Journal of Water and Wastewater Treatment*. **3** (2): 2381–5299. 10.16966/2381-5299.139.

[31] N. Amadou, E. Richard, N. Waingeh, I. Hélène, Y. Ndombow, and K. Jules-Roger. (2017). “Physicochemical and Sensory Properties of Ginger Spiced Yoghurt”. *Journal of Nutritional Therapeutics*. **6** (3): 68 –74. 10.6000/1929-5634.2017.06.03.2.

[32] J. N. Egila, B. E. N. Dauda, and T. Jimoh.

(2010). “Biosorptive removal of cobalt (II) ions from aqueous solution by Amaranthus hydridus L. stalk wastes”. *African Journal of Biotechnology*. **9** (48): 8192–8198. 10.5897/AJB10.1365.

[33] M. B. Desta. (2013). “Batch sorption experiments: Langmuir and freundlich isotherm studies for the adsorption of textile metal ions onto teff straw (eragrostis tef) agricultural waste”. *Journal of Thermodynamics*. **1** (1): 6–10. 10.1155/2013/375830.

[34] G. G. Kusse, M. Zewde, and A. A. Yoseph. (2019). “Determination of concentration of heavy metals in ginger using flame atomic absorption spectroscopy”. *African Journal of Plant Science*. **13** (6): 163–167. 10.5897/ajps2019.1787.

[35] R. Ahmad. (2009). “Studies on adsorption of crystal violet dye from aqueous solution onto coniferous pinus bark powder (CPBP)”. *Journal of Hazardous Materials*. **171** (1–3): 767–773. 10.1016/j.jhazmat.2009.06.060.

[36] H. Tounsadi, A. Khalidi, M. Abdennouri, and N. Barka. (2015). “Biosorption potential of Diplotaxis harra and Glebionis coronaria L. biomasses for the removal of Cd(II) and Co (II) from aqueous solutions”. *Journal of Environmental Chemical Engineering*. **3** (2): 822–830. 10.1016/j.jece.2015.03.022.

[37] K. M. S. Surchi. (2011). “Agricultural Wastes as Low Cost Adsorbents for Pb Removal: Kinetics, Equilibrium and Thermodynamics”. *International Journal of Chemistry*. **3** (3): 103–112. 10.5539/ijc.v3n3p103.

[38] T. Jimoh, J. N. Egila, B. E. N. Dauda, and Y. A. Iyaka. (2011). “Preconcentration and removal of heavy metal ions from aqueous solution using modified charcoal”. *Journal of Environmental Chemistry and Ecotoxicology*. **3** (9): 238–243.

[39] L. Xu, X. Zheng, H. Cui, Z. Zhu, J. Liang, and J. Zhou. (2017). “Equilibrium, Kinetic, and Thermodynamic Studies on the Adsorption of Cadmium from Aqueous Solution by Modified Biomass Ash”. *Bioinorganic Chemistry and Application*. **2017** : 1–9. 10.1155/2017/3695604.

[40] H. K. Boparai, M. Joseph, and D. M. O’Carroll. (2011). “Kinetics and thermodynamics of cadmium ion removal by adsorption onto nano zerovalent iron particles”. *Journal of Hazardous Materials*. **186** (1): 458–465. 10.1016/j.jhazmat.2010.11.029.

[41] A. Achmad, J. Kassim, T. K. Suan, R. C. Amat, and T. L. Seey. (2012). “Equilibrium, kinetic and thermodynamic studies on the adsorption of direct dye onto a novel green adsorbent developed from Uncaria gambir extract”. *Journal of Physical Science*. **23** (1): 1–13.

[42] V. C. Srivastava, I. D. Mall, and I. M. Mishra. (2008). “Removal of cadmium(II) and zinc(II) metal ions from binary aqueous solution by rice husk ash”. *Colloids and Surfaces A: Physicochemical and Engineering Aspects*. **312** (2–3): 172–184. 10.1016/j.colsurfa.2007.06.048.

[43] F. C. Wu, B. L. Liu, K. T. Wu, and R. L. Tseng. (2010). “A new linear form analysis of Redlich-Peterson isotherm equation for the adsorptions of dyes”. *Chemical Engineering Journal*. **162** (1): 21–27. 10.1016/j.cej.2010.03.006.

[44] F. Gimbert, N. Morin-Crini, F. Renault, P. M. Badot, and G. Crini. (2008). “Adsorption isotherm models for dye removal by cationized starch-based material in a single component system: Error analysis”. *Journal of Hazardous Materials*. **157** (1): 34–46. 10.1016/j.jhazmat.2007.12.072.

[45] F. Batool, J. Akbar, S. Iqbal, S. Noreen, and S. N. A. Bukhari. (2018). “Study of Isothermal, Kinetic, and Thermodynamic Parameters for Adsorption of Cadmium: An Overview of Linear and Nonlinear Approach and Error Analysis”. *Bioinorganic Chemistry and Applications*. **2018** (8): 205–212. 10.1155/2018/3463724.

[46] J. Twisk. (2010). “Basic statistical methods 4th ed”. Harper and Row, New York. 10.1093/acprof:oso/9780199561629.003.03.

[47] S. Arivoli, V. Marimuthu, and A. R. M. Jahangir. (2013). “Kinetics of batch adsorption of iron (II) ions from aqueous solution using activated carbon from

Strychnos nux-vomica L". *International Journal of Scientific & Engineering Research*. **4** (12): 407–417.

[48] B. Li, F. Zhou, K. Huang, Y. Wang, S. Mei, Y. Zhou, and T. Jing. (2016). "Highly efficient removal of lead and cadmium during wastewater irrigation using a polyethylenimine-grafted gelatin sponge". *Scientific Reports*. **6** (16): 573–581. 10.1038/srep33573.

[49] M. R. Kulkarni, T. Revanth, A. Acharya, and P. Bhat. (2017). "Removal of Crystal Violet dye from aqueous solution using water hyacinth: Equilibrium, kinetics and thermodynamics study". *Resource-Efficient Technologies*. **3** (1): 71–77. 10.1016/j.reffit.2017.01.009.

[50] G. M. Al-Senani and F. F. Al-Fawzan. (2018). "Adsorption study of heavy metal ions from aqueous solution by nanoparticle of wild herbs". *Egyptian Journal of Aquatic Research*. **44** (3): 187–194. 10.1016/j.ejar.2018.07.006.

[51] K. L. Wasewar. (2010). "Adsorption of metals onto tea factory waste: A review". *Ijrras*. **3** (3): 303–322.

[52] H. S. Mohamed, N. K. Soliman, D. A. Abdelrheem, A. A. Ramadan, A. H. Elghandour, and S. A. Ahmed. (2019). "Adsorption of Cd 2+ and Cr 3+ ions from aqueous solutions by using residue of Padina gymnospora waste as promising low-cost adsorbent". *Heliyon*. **5** (3): 106–111. 10.1016/j.heliyon.2019.e01287.

[53] R. Ahmad and S. Haseeb. (2016). "Kinetic, isotherm and thermodynamic studies for the removal of Pb2+ ion by a novel adsorbent Luffa acutangula (LAPR)". *Desalination and Water Treatment*. **57** (38): 17826–17835. 10.1080/19443994.2015.1088476.

[54] K. A. Rahman, W. S. Loh, and K. C. Ng. (2013). "Heat of adsorption and adsorbed phase specific heat capacity of methane/activated carbon system". *Procedia Engineering*. **56** (13): 118–125. 10.1016/j.proeng.2013.03.097.

[55] Y. T. Gebreslassie. (2020). "Equilibrium, Kinetics, and Thermodynamic Studies of Malachite Green Adsorption onto Fig (Ficus cartia) Leaves". *Journal of Analytical Methods in Chemistry*. **2020** : 103–108. 10.1155/2020/7384675.

[56] M. J. Keenan, J. Zhou, M. Hegsted, C. Pelkman, H. A. Durham, D. B. Coulon, and R. J. Martin. (2015). "Role of resistant starch in improving gut health, adiposity, and insulin resistance". *Advances in Nutrition*. **6** (2): 198–205. 10.3945/an.114.007419.

[57] K. A. Steinmetz and J. D. Potter. (1996). "Vegetables, Fruit, and Cancer Prevention". *Journal of the American Dietetic Association*. **96** (10): 1027–1039. 10.1016/S0002-8223(96)00273-8.

[58] M. A. Njoki, G. Mercy, G. Nyagah, and A. Gachanja. (2016). "Fourier Transform Infrared Spectrophotometric Analysis of Functional Groups found in Ricinus Communis L. and Cucurbita Maxima Lam. Roots, Stems and Leaves as Heavy Metal Adsorbents". *International Journal of Science*. **5** (3): 861–871.

[59] C. E. Osakwe, I. Sanni, S. Sa'id, and A. Zubairu. (1997). "Adsorption of Heavy Metals from Wastewaters Using Adonosia digitata Fruit Shells and Theobroma cacao Pods as Adsorbents: A Comparative Study". *Au Journal of Technology*. **18** (1): 11–18.

[60] M. H. Gohil and S. J. Verma. (2012). "Scanning electron microscopy study to analyze the morphological characteristics of root surfaces after application of Carisolv gel in association with scaling and root planing: In vitro study". *Journal of Indian Society of Periodontology*. **16** (3): 329–332. 10.4103/0972-124X.100906.